HHS Public Access

Author manuscript

Curr Cardiovasc Imaging Rep. Author manuscript; available in PMC 2018 June 01.

Published in final edited form as:

Curr Cardiovasc Imaging Rep. 2017 January ; 10(1): . doi:10.1007/s12410-017-9397-1.

Molecular Imaging of Atherosclerosis: A Clinical Focus

Mohammed M. Chowdhury, MD, MRes, MSc, MRCS[a], **Ahmed Tawakol, MD**[b], and **Farouc A. Jaffer, MD, PhD**[b]

[a]Division of Vascular & Endovascular Surgery, Department of Surgery, University of Cambridge and Cambridge University Hospitals, Cambridge, UK

[b]Division of Cardiology, Massachusetts General Hospital; Harvard Medical School; Boston, Massachusetts

Abstract

Molecular imaging of cardiovascular disease is a powerful clinical and experimental approach that can inform our understanding of atherosclerosis biology. Complementing cross-sectional imaging techniques that provide detailed anatomical information, molecular imaging can further detect important biological changes occurring within atheroma, and refine the prediction of vascular complications. In addition, molecular imaging of atherosclerosis can illuminate underlying pathophysiology and serve as a surrogate end-point in clinical trials of new drugs. This review showcases promising molecular approaches for imaging atherosclerosis, with a focus on PET, MRI, and intravascular near-infrared fluorescence (NIRF) imaging methods that are in the clinic or close-to-clinical usage.

Keywords

atherosclerosis; molecular imaging; positron emission tomography; near-infrared fluorescence; optical coherence tomography

Introduction

Atherosclerosis-induced cardiovascular disease is a major global health problem and a major cause of death in every region of the world (1). In clinical practice, anatomical imaging modalities such as computed tomography (CT), ultrasound (US) and magnetic resonance imaging (MRI) are essential to delineate vascular anatomy and diagnose atherosclerosis stenosis severity, but do not routinely provide information about underlying pathophysiological processes driving the disease and its consequences. Advances in molecular atherosclerosis imaging research provide opportunities to explore pathological

Corresponding Author: Farouc Jaffer MD PhD, MGH Cardiovascular Research Center, Cardiology Division, 185 Cambridge Street, Simches 3206., Boston, Massachusetts, USA, fjaffer@mgh.harvard.edu, Tel: + 1 617 724 9353 Fax: +1 617 860 3180.

Compliance with Ethics Guidelines

Human and Animal Rights and Informed Consent

This article does not contain any studies with human or animal subjects performed by any of the authors.

Conflict of Interest

Mohammed M. Chowdhury declares that he has no conflict of interest.

mechanisms occurring at the cellular level and within the vessel wall. When applied to studying atherosclerosis, nuclear imaging with positron emission tomography (PET) has the potential to detect early vascular changes, prior to the onset of clinical symptoms or even before angiographically-detectable luminal stenosis. In addition, cross-sectional multi-modal imaging using combined PET/CT or PET/MRI systems offers great potential to incorporate anatomical, functional and molecular datasets. Furthermore, catheter-based near-infrared fluorescence imaging (NIRF) molecular imaging has enabled high-resolution insights into atherosclerosis progression, stent restenosis, and stent thrombosis. This review will highlight promising novel approaches, with a focus on recent advances in the literature.

Positron Emission Tomography

Positron emission tomography (PET) produces three-dimensional quantitative images of the distribution of a positron-emitting radionuclide. PET typically images functional processes in the body, developing applications in areas such as oncology, cardiology, and neurology. PET is based on the radioactive decay of positron-emitter isotopes by beta plus decay. Among the positron-emitting isotopes which can be produced, the most commonly used in PET are those having a short half-life and which are present naturally in many biological compounds, such as ^{11}C, ^{18}F, ^{15}O, and ^{13}N.

The most common radiopharmaceutical in PET is 2-[^{18}F] fluoro-2-deoxy-D-glucose (^{18}F-FDG), a compound which was first administered to patients in the late 1970's, and now utilized in over 90% of clinical PET scans. It is an analogue of glucose allowing quantitation of glucose metabolism, and it is most commonly used for cancer detection, staging, and monitoring, being considered the gold standard for the *in vivo* assessment of many tumour types.

When a positron is emitted from the nucleus, it travels a short distance (typically 1–2 mm) until it collides with an electron. The positron-electron collision results in an annihilation event, which produces radiation in the form of two photons, each with an energy of 511 keV, emitted in opposed directions. PET detection systems are poised to identify the coincidentally emitted photon pairs, and reconstructs the line from which they originated (hence enabling quantification of tissue activity). A common measure of PET tracer uptake is the standardized uptake value (SUV). The SUV is a semi-quantitative measure, subsequently adjusted for injected tracer dose and body weight. When SUV is corrected for blood pool activity (the circulating level of tracer in the venous system), the target-to-background ratio (TBR) is derived. Ongoing work is establishing the relative merits of SUV and TBR measures in PET characterization of atherosclerosis (2).

FDG PET molecular imaging of inflammation in atherosclerosis—

Fluorodeoxyglucose (18F-FDG) is a radiolabeled glucose analogue that is taken up by all glucose-metabolizing cells. Once internalized, it becomes metabolically trapped, and accumulates in direct proportion to the tissue rate of glycolysis. By exploiting the glucose-dependent metabolism of macrophages in atherosclerosis, FDG PET can illuminate macrophage burden *in vivo* (3–5).

Initial clinical studies: Rudd *et al.* performed the first prospective validation study of using FDG detect and quantify atheroma inflammation (5). The authors observed significantly higher FDG tracer uptake within symptomatic carotid plaques when compared to the contralateral asymptomatic carotid artery. Histological validation was performed in a second key study, in which PET imaging was performed on individuals scheduled for endarterectomy, and FDG uptake quantified from those images was later compared to detailed immunohistochemical analysis of the excised plaque specimens (6). Quantitative analysis subsequently revealed that the intensity of the FDG uptake correlated well with the macrophage content of plaque specimens ($r=0.70$, $p<0.001$) (Figure 1). These pivotal studies established the utility of FDG to assess plaque inflammation, with subsequent applications to understanding atherosclerosis pathophysiology and to assessing pharmacotherapies.

Relationship of FDG uptake to other plaque constituents: Carotid artery FDG uptake has also been shown to relate to the extent of neovascularization, a marker of plaque hypoxia – implicated in pathogenesis of the unstable atherosclerotic plaque (7). In a recent study by Taqueti *et al*, patients undergoing carotid endarterectomy underwent 18F-FDG PET/CT imaging prior to surgery. The endarterectomy specimens were then analyzed for macrophage content (CD68), activated inflammatory cells (MHC class II) and microvessels (CD31). Increased FDG uptake was observed in inflamed plaque regions as demonstrated in earlier studies but the authors also observed increased FDG uptake in areas of increased microvascular permeability, perfusion and microvascularization – possibly implicating positive uptake in areas that are linked to unstable plaque. Pathophysiologically, the presence of neovasculature may facilitate delivery of FDG to metabolically active cells.

FDG uptake in atherosclerotic specimens has also been linked to plaque hypoxia. (4) A recent study provided insights into the relationship between hypoxia and macrophage content and function. That study demonstrated that hypoxia triggered increased pro-inflammatory activity by macrophages, via a HIF-1 alpha-dependent mechanism. Furthermore, the study showed that glycolytic flux remained closely related monocyte pro-inflammatory actions (e.g. TNF alpha production), regardless of whether or not hypoxia was present (8). Hence, the amount of FDG that accumulates within macrophages is influenced not only the number of inflammatory cells, but also their pro-inflammatory phenotype, which can be impacted by hypoxia as well as other factors.

Arterial FDG signal as a predictor of atherosclerotic disease progression and clinical events: Moustafa *et al.* examined the role of 18F-FDG PET/CT in patients with symptomatic carotid disease (9). They identified a positive correlation between microembolic signals identified from transcranial Doppler and carotid FDG uptake on PET/CT. Notably, the percent luminal stenosis did not differentiate plaques that produced microemboli (10). Similarly, cross-sectional studies revealed that both aortic and coronary arterial FDG uptake increase after myocardial infarction (11).

The arterial FDG signal can also predict the progression of underlying atheroma. Abdelbaky et al observed that atheromatous plaques with high FDG uptake subsequently undergo more rapid atherosclerotic progression (measured as incident arterial calcification) compared to arterial locations with lower amounts of FDG uptake (12). Another study demonstrated that

early changes in arterial FDG uptake predict later changes in plaque progression (plaque thickness, by MRI) (13).

Moreover, the arterial FDG signal has been repeatedly shown to be an independent predictor of future atherothrombotic disease events. Rominger *et al.* first showed, in a population of individuals with oncologic diagnoses, that the arterial FDG signal predicts subsequent CVD events (14). Extending those findings, Figueroa *et al.* studied individuals without active cancer, and found that the arterial FDG signal independently predicted CVD events beyond coronary artery calcium measures or clinical risk scores (such as the Framingham Risk Score) (15) (Figure 2). Small prospective studies have demonstrated a similar relationship between arterial FDG uptake and subsequent CVD (16).

FDG PET assessment of anti-atherosclerosis pharmacotherapeutics: Given that the FDG signal is reproducible (17), and that its modulation predicts atherosclerotic disease progression (13), it is ripe for use as a biomarker to examine novel therapies. Indeed, several studies have assessed the impact of anti-inflammatory pharmacotherapy on the FDG signal. A question of substantial importance is whether the directional changes seen in the PET signal relate to directional changes seen in clinical endpoint evaluations in the context of pharmacotherapy. To date, insights are emerging from trials of 5 therapeutic compound classes for which there are both FDG PET as well as clinical endpoint trial data.

The first such drug class is statins. Several groups have shown that statins are associated with reduction is in arterial FDG uptake (18,19), findings that are undoubtedly in line with reductions in CVD events imparted by statins (20). Interestingly, the magnitude of signal reduction might also be important. High-dose statins have a 2-fold greater impact on the arterial signal compared to low dose statins (19), a finding that is concordant with the observation that high dose statins reduce CVD events roughly twice as well as low dose statins. Similarly, the thiazolidinedione, pioglitazone, was found to significantly reduce arterial FDG uptake in diabetic patients (21). Likewise, TZDs have been shown to reduce CVD events in this population (22).

On the other hand, a lack of change in the arterial FDG signal may forecast a lack of therapeutic efficacy. Fayad *et al* (23) demonstrated that dalcetrapib (a modulator of cholesteryl ester transfer protein activity) did not reduce any of the pre-specified FDG-PET measures. Likewise, dalcetrapib failed to improve clinical outcomes in a large outcomes trial (24). More recently, a selective inhibitor of lipoprotein phospholipase A2 was assessed using arterial FDG PET imaging, and was found to be ineffective at reducing the FDG signal (25). Concordantly, Lp-PLA2 inhibitors have subsequently been found to be ineffective in reducing CVD events (26, 27). Most recently, the results of both imaging and clinical outcomes trials of drugs targeting p38 MAP Kinase have been reported. One PET study reported no change in the signal, when the pre-defined endpoints were used, but identified a possible reduction in the signal using an exploratory endpoint (28). However, a subsequent study found no reduction in the PET signal using any of the measured FDG endpoints (29). A subsequent trial of p38 MAPK antagonism on CVD events subsequently found no benefit (30). Thus, for all 5 drug classes for which there are both imaging and clinical endpoint trial data, there has been concordance between the pre-specified imaging results and clinical end-

point results. Accordingly, arterial FDG PET imaging, when used in Phase II trials, may be used to identify drugs with greater likelihood for success in Phase III studies.

FDG PET molecular imaging of inflammation in abdominal aortic aneurysm (AAA)—Inflammation is a key driver of AAA expansion and rupture, and the ability to assess AAA inflammation could improve risk stratification and motivate specific anti-inflammatory therapies. A small number of studies have explored the utility of FDG-PET/CT imaging to characterize AAA. One pilot study of 26 patients with AAA using suggested a possible positive correlation between 18F-FDG uptake and aneurysmal growth rate and rupture (31). In contrast, a relatively brief longitudinal observational study (32) of 39 patients with small-to-medium size AAA failed to replicate those findings (in fact there was in inverse association between tracer uptake change in AAA diameter). However, it should be noted that very few subjects experienced progression of AAA diameter in that study, likely due to the relatively short follow up period (of only 9 months). Since AAA diameters tend to enlarge at a rate of 2–3 mm per year (33), a 9-month follow period employed in that study may have been insufficient to robustly test the hypothesis. Accordingly, the relationship between FDG uptake in AAA and subsequent AAA behavior remains unclear and requires further investigation.

FDG PET molecular imaging of inflammation in peripheral atherosclerosis—Relatively few molecular imaging studies have focused attention on the lower limb arterial tree. This may be due to the fact that those vessels tend to be relatively small, and that atherosclerotic inflammation may play a less important role in the lower limb atherosclerosis. The available data are derived from studies using multiple different tracers assessing: perfusion (including ^{15}O-water, $C^{15}O_2$, $^{15}O_2$, ^{13}N-ammonia), angiogenesis (including ^{76}Br-nanoprobe, ^{68}Ga-NOTA-RGD, ^{64}Cu-DOTA-CANF-comb, ^{64}Cu-DOTA-VEGF) or atherosclerosis (including ^{18}F-FDG, ^{18}F-sodium fluoride, ^{11}C-acetate, ^{64}Cu-DOTA-CANF) (34, 35). Studies have also compared FDG uptake in peripheral vessels using PET/CT and PET/MRI in carotid and peripheral vessels (36). Silvera *et al.* demonstrated that both imaging modalities accurately identified areas of lipid-rich plaques more often than collagen-rich or calcified plaques.

PET molecular imaging of plaque osteogenic activity (active calcification)—Cardiovascular calcification is associated with an increased risk of vascular events (37). Specifically, coronary artery calcification score (CAC) is now widely used to refine the prediction of future coronary artery events including myocardial infarction and cardiac death (38). Although vascular wall calcification seen on CT is considered a powerful surrogate risk factor for poor cardiovascular outcome, it represents the end stage of the overall calcification process (39). New approaches using PET CT imaging to assess the active calcification stage might improve risk prediction further and offer an opportunity to initiate directed anti-atheroma therapy earlier.

18F Sodium fluoride molecular imaging of plaque osteogenesis/microcalcification: The tracer 18F-sodium fluoride (18F-NaF) typically deposits in bone where the fluoride ions undergo rapid exchange with the hydroxyl group (-OH) on the surface of the hydroxyapatite

matrix to form fluoroapatite (40). As such, its primary clinical application has been in the evaluation of primary and metastatic bone tumors (41). A major advantage of 18F-NaF is the lack of myocardial background compared to FDG, allowing high conspicuity of 18F-NaF+ coronary lesions. More recent interest has focused on its role in identifying areas of active microcalcification within the cardiovascular system, and specifically in atherosclerosis where it is believed that microcalcification may play a role in plaque rupture through both mechanical and inflammatory effects.

Initial clinical studies: Prior studies established a strong link between chronic inflammation and the subsequent development of soft tissue calcification in atherosclerosis (42). Clinically, Derlin *et al* (43) first described correlations and distinct differences across plaques whilst imaging with FDG and 18F-sodium fluoride, and found overlap of the two tracers in only 6.5% of plaques of various arterial beds, suggesting each tracer reports on different plaque pathological processes. Abdelbaky *et al*. evaluated 137 patients by determining the degree of aortic inflammation using 18F-FDG PET/CT scanning, and found that higher levels of inflammation were significantly associated with subsequent CT-calcification over a 5-year period (44).

Derlin *et al*. further demonstrated the potential to image to early-stage, or "active," microcalcification in atherogenesis using 18F-NaF in human carotid plaques (45). In a key study, this work was extended into the human coronary artery domain by Dweck and Newby (46), who demonstrated outstanding signal-to-noise of NaF uptake in coronary plaques (Figure 3). In a landmark study, Dweck and colleagues further demonstrated the value of 18F-NaF to prospectively demonstrate that high 18F-NaF uptake was associated with high-risk, often ruptured carotid and coronary lesions, with histological evidence of active calcification, macrophages, necrosis, and apoptosis (47). A recent retrospective study by Fiz *et al*. (48) further assessed the correlation between calcification density (as assessed by CT, in Hounsfield units) and 18F-NaF uptake within the infrarenal aorta of oncology patients. There was a significant inverse correlation between 18F-NaF uptake and macrocalcification, supporting the concept that 18F-NaF may act as a valid marker of calcium deposition primarily in the early stages of plaque formation.

Recently, detailed mechanistic studies of NaF tracer selectivity, specificity, and pharmacodynamic behavior have been performed, in vitro and in human carotid plaques (49). Irkle et al. demonstrated that 18F-NaF adsorbs to calcified deposits within plaque and is highly selective and specific, and further noninvasively detects areas of microcalcification that are associated with active unstable atherosclerosis. To this effect, 18F-NaF co-localized to areas of nascent calcification and could mark a novel non-invasive biomarker of the high-risk pathology. Furthermore, the study has suggested that adsorption is dependent primarily on surface area, consistent with the notion that the complex surface of microcalcifications allows more binding.

18F-NaF PET and outcome studies: A molecular imaging modality that identifies early active microcalcification and allied inflammatory processes within atherosclerotic plaques could allow for a refined understanding of plaque vulnerability and prediction of lesion-specific or artery-specific hard events such as myocardial infarction, stroke, and sudden

death. In the next several years, outcome studies are anticipated, including a multicenter observational study 18F-NaF PET as a marker of coronary plaque vulnerability to detect culprit and non-culprit unstable coronary plaques in patients with recent myocardial infarction (NCT02278211 at Clinicaltrials.gov). The investigators plan to follow these patients to determine the prognostic significance of coronary 18F-NaF uptake. A key question is whether 18F-NaF will offer significant predictive ability beyond the traditional calcium marker of coronary artery calcium (CAC) scoring, which has an established role in risk prediction in the primary prevention CAD population.

Alternate PET tracers—An important limitation of coronary FDG imaging is that the coronary plaque signal may be overwhelmed by high myocardial uptake. Therefore, the search for additional PET tracers that assess vascular inflammation remains important. 68Ga-DOTATATE ({1,4,7,10-tetraazacyclododecane-*N, N′, N″, N‴*-tetraacetic acid}-D-Phe(1), Tyr(3)-octreotate)) has specific binding capabilities for the somatostatin receptor subtype 2. It has been demonstrated that in retrospective studies there is positive uptake of this tracer in coronary arteries (50), as well uptake aorta, iliac, and carotid vessels (51). 68Ga-DOTATATE offers a coronary imaging advantage as there is minimal uptake in the myocardium, in distinction to FDG. Positive 64Cu-DOTATATE uptake in human carotid plaques further correlates with cellular markers of inflammation (CD68 and CD163) (52). Furthermore, in a comparison with a similar somatostatin analogue tracer, 68Ga-DOTATOC, 68Ga-DOTATATE correlated better with inflamed arteries alongside traditional cardiovascular risk factors – suggesting a potential role in atherosclerotic disease assessment (53). Prospective validation is, however, warranted.

11C-PK11195 targets the translocator protein (TSPO) on the macrophage surface. Its use in vascular imaging is challenging due to the shorter half-life of carbon 11 (20 minutes), but it has been utilized as a marker of plaque inflammation, particularly in the carotid circulation (54, 55). An advantage of this tracer is the significant correlation between 11C-PK11195 uptake ratio and autoradiographic measurement of translocator protein binding sites (55).

18F-fluorodeoxymannose (FDM) is an isomer of glucose, and has been postulated to be expressed on the M2 (more reparative) subtype of macrophages. Its use in research has been limited to preclinical animal work (56) – yet further work may be published once radiolabeling becomes simpler. Nonetheless, Tahara *et al* proposed that as supported by *in vitro* investigations, FDM had a 35% higher uptake compared to FDG, based on lower inhibition of hexokinase activity – suggesting it may be more specific for areas of acute inflammation. Further investigation, including feasibility of clinical FDM imaging, is required to understand if FDM can provide additional or complementary clinical value in comparison to FDG in risk prediction.

Ultrasmall Superparamagnetic Iron Oxide Nanoparticle-enhanced MRI

Ultrasmall superparamagnetic iron oxide (USPIO) nanoparticles are a well-established class of dextran-based MRI agents that report on phagocytic cellular activity. Several preparations have been clinically tested and one preparation, feurmoxytol, is FDA-approved as replacement therapy for iron-deficient chronic kidney disease patients. With regards to

atherosclerosis imaging, intravenously administered long-circulating UPSIO nanoparticles are eventually taken up by macrophages and thus allow visualization of macrophage-laden plaque. Their properties allow direct imaging on T2-weighted MRI sequences, where they induce a loss of MR signal.

USPIO-enhanced molecular MRI can assess inflammatory plaque burden in aortic aneurysms, carotid artery disease, myocardial infarction and response to pharmacotherapy. Kooi *et al* (57) first demonstrated successful histologically-confirmed USPIO (ferumoxtran) MRI of macrophage content in carotid plaque rupture-prone zones of patients undergoing carotid endarterectomy (validated with histology and electron microscopy). In a unique clinical trial, the ATHEROMA Study (58) provided new insights into the comparative of efficacy of low potency vs. high-potency statin therapy in attenuating plaque macrophages in patients. The authors evaluated the effects of low-dose (10mg) and high-dose (80mg) atorvastatin therapy on carotid plaque inflammation in 47 patients and demonstrated a significant reduction in UPSIO-defined inflammation in patients receiving high dose statin therapy ($p=0.0003$). Currently, long circulating USPIOs such as ferumoxtran are not routinely clinically available, which has limited USPIO MRI atherosclerosis imaging studies in recent years.

However, new data has emerged by repurposing FDA-approved ferumoxytol for molecular MRI. One study (59) investigated UPSIO MRI imaging in patients suffering a myocardial infarction and demonstrate areas of increased USPIO uptake in acute infarction as well as remote myocardium ($n=16$; $p<0.001$). Further work is required to assess its range of applications in the acute setting. In addition, in comparative studies with 18F-FDG PET, USPIO ferumoxytol MRI identified vascular inflammation reliably in abdominal aortic aneurysms yet subtle differences compared to FDG suggest that inflammatory cell phocytosis and glycolysis may not exactly coincide (60). As ferumoxytol is a weaker T2 MRI contrast agent than ferumoxtran, it is not clear that ferumoxytol is strong enough to allow assessment of inflammation in smaller targets than the heart or aorta, such as carotid or coronary atheroma.

High-resolution Molecular Imaging Via Intravascular Near-Infrared Fluorescence Imaging

Optical imaging using near-infrared fluorescence (NIRF) light is an emerging imaging technique delivering high sensitivity and the ability to be employed to image a wide range of molecular entities *in vivo*, via a versatile fluorescent probe design (61–63). The use of NIR wavelengths allows deeper photon penetration into tissue and reduced tissue autofluorescence, resulting in higher sensitivity to detect exogenous NIR fluorophores (molecular imaging agents). Greater depth can be probed in the far-red or near-infrared spectral region as the absorption is as at least one order of magnitude lower than in the visible range. NIR light (650–900nm wavelength) can penetrate several centimeters into tissue. Furthermore, as optical imaging is routine in the cardiac catheterization laboratory (via intravascular optical coherence tomography), intravascular NIRF offers a promising translational approach into clinical coronary arterial imaging. Excitingly, the first human intravascular NIRF imaging study was recently performed and demonstrated the ability to sensitively to detect NIR autofluorescence in human coronary arteries (64). This study paves

the way forward for targeted intravascular NIRF molecular imaging studies in coronary patients.

Given the favorable high sensitivity in the NIR window, NIRF imaging can further enable signal detection through blood. The first real-time catheter molecular sensing probe was first described by Jaffer *et al* (65), who detected in vivo inflammatory cysteine protease activity in experimental atheroma of human-sized arteries. The first rotational, automated 2D imaging catheter was engineered by Jaffer *et al* (66) and intra-arterial imaging of stented rabbit aortas and coronary bare-metal stents demonstrated excellent nanomolar sensitivity to fluorophores to image plaque and stent injury-induced arterial inflammation. Further research into this novel imaging approach will also target key molecules in in atherosclerosis (i.e. OxLDL, acetylated LDL, MMPs). Recently for example, Khamis *et al* (67) developed an antibody-based NIRF approach for targeting oxLDL *in vivo* – providing new potential avenues for exploring molecular compositions of atheroma longitudinally with intravascular NIRF imaging.. In addition, FDA-approved indocyanine green is a promising translational NIR fluorophore for plaque imaging (68), and has recently been shown to report on impaired endothelial barrier function in human plaques (69).

One limitation to standalone NIRF imaging is the lack of co-registration (analogous to PET imaging without CT/MR anatomical information). One potential exciting approach is dual-modality NIRF-optical coherence tomography (OCT). This concept has been translated into an intravascular imaging system (70) (Figure 4), and revealed the ability to successfully co-localise microstructural and biological imaging data. Characterization *in vivo* of inflammatory cells using OCT can quantify molecular expression and activity using cathepsin protease-activated NIR molecular beacons. Furthermore, stent-induced injury (fibrin deposition in restenosis injury, platelet deposition and inflammatory endothelial infiltration) can be quantified and investigated using this single pullback technology (71). Attesting to the translational potential of NIRF-OCT, an intravascular NIRF-OCT system reporting on NIR autofluorescence has been recently performed in the coronary arteries of patients (64). Further research into its clinical implications and translation is required – yet the high-resolution information that such multi-modality imaging offers has the potential to transform coronary arterial molecular imaging of atherosclerosis.

Conclusions and Future Directions

Current risk stratifications in a number of vascular conditions are based primarily on anatomical data such as stenosis or calcium score. The advent of new molecular imaging techniques, including PET/CT and intravascular high-resolution NIRF-OCT, could enhance the identification of high-risk plaques, arteries, and patients harboring plaque inflammation or other pathobiology. These technologies, in particular FDG PET, have made significant clinical inroads into assessing atheroma pharmacotherapeutic efficacy in Phase II clinical trials. Furthermore, development of novel tracers will enhance in vivo assessment of key pathobiological processes including inflammation, hypoxia and neoangiogenesis. The overarching question is whether such imaging techniques will improve our understanding of human plaque biology and ultimately the risk of plaque complication and restenosis, to identify better those patients where such vascular events can be pre-empted utilizing tailored

systemic and/or local therapies. Given the ongoing translation of new imaging agents and new imaging devices, the future for atherosclerosis molecular imaging appears bright.

Acknowledgments

Ahmed Tawakol reports grants and personal fees from Takeda, grants and personal fees from Actelion, grants from Genetech, and personal fees from Astra Zeneca, outside the submitted work.

Farouc A. Jaffer reports grants from Canon, grants from Siemens, personal fees from Abbott vascular, personal fees from Boston Scientific, outside the submitted work. In addition, Dr. Jaffer has a patent for Intravascular NIRF imaging with royalties paid to Canon.

Disclosures: Dr. Jaffer has received research funding from Siemens and Canon, and has a consulting agreement with Boston Scientific and Abbott Vascular. Massachusetts General Hospital has a patent licensing arrangement with Canon Corporation. Dr. Jaffer has the right to receive licensing royalties through this licensing arrangement. Dr. Tawakol has received research funding from Actelion, Genetech, and Takeda, and has a consulting agreement with Actelion.

Support Sources: M.M.C is supported by the Royal College of Surgeons of England Fellowship Programme and British Heart Foundation Research Fellowship award FS/16/29/31957. F.A.J is supported by NIH R01HL122388 (F.A.J) and the MGH Hassenfeld Research Scholar Fund. A.T is supported by NIH R01HL122177-(AT).

References

Papers of particular interest, published recently, have been highlighted as:

* Of importance

** Of outstanding importance

1. Naghavi M, Wang H, Lozano R, et al. GBD 2013 Mortality and Causes of Death Collaborators. Global, regional, and national age-sex specific all-cause and cause-specific mortality for 240 causes of death, 1990–2013: a systematic analysis for the Global Burden of Disease Study 2013. Lancet. 2015; 385:117–171. [PubMed: 25530442]
2. Chen W, Dilsizian V. PET assessment of vascular inflammation and atherosclerotic plaques: SUV or TBR? J Nucl Med. 2015; 56:503–504. [PubMed: 25722451]
3. Tarkin JM, Joshi FR, Rudd JH. PET imaging of inflammation in atherosclerosis. Nat Rev Cardiol. 2014; 11:443–457. [PubMed: 24913061]
4. Folco EJ, Sheikine Y, Rocha VZ, et al. Hypoxia but not inflammation augments glucose uptake in human macrophages: Implications for imaging atherosclerosis with 18flourine-labeled 2-deoxy-D-glucose positron emission tomography. J Am Coll Cardiol. 2011; 58:603–614. [PubMed: 21798423]
5. Rudd JH, Warburton EA, Fryer TD, et al. Imaging atherosclerotic plaque inflammation with [18F]-fluorodeoxyglucose positron emission tomography. Circulation. 2002; 105:2708–2711. [PubMed: 12057982]
6. Tawakol A, Migrino RQ, Bashian GG, et al. In vivo 18F-fluorodeoxyglucose positron emission tomography imaging provides a noninvasive measure of carotid plaque inflammation in patients. J Am Coll Cardiol. 2006; 48:1818–1824. [PubMed: 17084256]
7. Taqueti VR, Di Carli MF, Jerosch-Herold M, et al. Increased microvascularisation and vessel permeability associate with active inflammation in human atheromata. Circ Cardiovasc Imaging. 2014; 7:920–929. [PubMed: 25170063]
*8. Tawakol A, Singh P, Mojena M, et al. HIF-1alpha and PFKFB3 mediate a tight relationahip between proinflammatory activation and anaerobic metabolism in atherosclerotic macrophages. Arterioscler Thromb Vasc Biol. 2015; 35:1463–1471. Findings in human, murine and animal models verify that hypoxia potentiates macrophage glycolytic flux, with an upregulation of proinflammatory activity. [PubMed: 25882065]

9. Moustafa RR, Izguierdo-Garcia D, Fryer TD, et al. Carotid plaque inflammation is associated with cerebral microembolism in patients with recent transient ischaemic attack or stroke: a pilot study. Circ Cardiovasc Imaging. 2010; 3:536–541. [PubMed: 20639303]

10. Marnane M, Merwick A, Sheehan OC, et al. Carotid plaque inflammation on 18F-fluorodeoxyglucose positron emission tomography predicts early stroke recurrence. Ann Neurol. 2012; 71:709–718. [PubMed: 22461139]

11. Rogers IS, Nasir K, Figueroa AL, et al. Feasibility of FDG imaging of the coronary arteries: comparison between acute coronary syndrome and stable angina. JACC Cardiovasc Imaging. 2010; 3:388–397. [PubMed: 20394901]

12. Abdelbaky A, Corsini E, Figueroa AL. Focal arterial inflammation precedes subsequent calcification in the same location: a longitudinal FDG-PET/CT study. Circ Cardiovasc Imaging. 2013:747–754. [PubMed: 23833282]

13. Joseph P, Ishai A, Mani V, et al. Short-term changes in arterial inflammation predict long-term changes in atherosclerosis progression. Eur J Nucl Med Mol Imaging. 2016 [In Press].

14. Rominger A, Saam T, Wolpers S, et al. 18F-FDG PET/CT identifies patients at risk for future vascular events in an otherwise asymptomatic cohort with neoplastic disease. J Nucl Med. 2009; 50:1611–1620. [PubMed: 19759117]

15. Figueroa AL, Abdelbaky A, Truong QA, et al. Measurements of arterial activity on routine FDG PET/CT images improves prediction of risk of future CV events. JACC Cardiovasc Imaging. 2013; 6:1250–1259. [PubMed: 24269261]

16. Marnane M, Merwick A, Sheehan OC, et al. Carotid plaque inflammation on 18F-fluorodeoxyglucose positron emission tomography predicts early stroke recurrence. Ann Neurol. 2012; 71:709–718. [PubMed: 22461139]

17. Rudd JH, Myers KS, Bansilal S, et al. (18)Fluorodeoxyglucose positron emission tomography imaging of atherosclerotic plaque inflammation is highly reproducible: implications for atherosclerosis therapy trails. J Am Coll Cardiol. 2007; 50:892–896. [PubMed: 17719477]

18. Tahara N, Kai H, Ishibashi M, et al. Simvastatin attenuates plaque inflammation: evaluation by fluorodeoxyglucose positron emission tomography. J Am Coll Cardiol. 2006; 48:1825–1831. [PubMed: 17084257]

19. Tawakol A, Fayad ZA, Mogg R, et al. Intensification of statin therapy results in a rapid reduction in atherosclerotic inflammation: results of a multicentre fluorodeoxyglucose-positron emission tomography/computed tomography feasibility study. J Am Coll Cardiol. 2013; 62:909–917. [PubMed: 23727083]

20. Baigent C, Blackwell L, et al. Cholesterol Treatment Trialists' (CCT) Collaboration. Efficacy and safety of more intensive lowering of LDL cholesterol: a meta-analysis of data from 170,000 participants in 26 randomised trials. Lancet. 2010; 376:1670–1681. [PubMed: 21067804]

21. Mizoguchi M, Tahara N, Tahara A, et al. Pioglitazone attenuates atherosclerotic plaque inflammation in patients with impaired glucose tolerance or diabetes a prospective, randomized, comparator-controlled study using serial FDG PET/CT imaging study of carotid artery and ascending aorta. JACC Cardiovasc Imaging. 2011; 4:1110–1108. [PubMed: 21999871]

22. Dormandy JA, Charbonnel B, Eckland DJ, et al. Secondary prevention of macrovascular events in patients with type 2 diabetes in the PROactive Study (PROspective pioglitazone Clinical Trial in macroVascular Events): a randomised controlled trial. Lancet. 2005; 366:1279–1289. [PubMed: 16214598]

**23. Fayad ZA, Mani V, Woodward M, et al. Safety and efficacy of dalcetrapib on atherosclerotic disease using novel non-invasive multimodality imaging (dal-PLAQUE): a randomised clinical trial. Lancet. 2011; 378:1547–1559. This landmark FDG PET/CT clinical study demonstrated that dalcetrapib did not reduce inflammation in human atheroma. The subsequent clinical outcomes study was neutral. [PubMed: 21908036]

24. Schwartz GC, Olsson AG, Abt M, et al. Effects of dalcetrapib in patients with a recent acute coronary syndrome. N Engl J Med. 2012; 367:2089–2099. [PubMed: 23126252]

25. Tawakol A, Singh P, Rudd JH, et al. Effect of treatment for 12 weeks with rilapladib, a lipoprotein-associated phospholipase A2 inhibitor, on arterial inflammation as assessed with 18F-

fluorodeoxyglucose-positron emission tomography imaging. J Am Coll Cardiol. 2014; 63:86–88. [PubMed: 23973698]

26. White HD, Held C, et al. STABILITY Investigators. Darapladib for preventing ischemic events in stable coronary heart disease. N Engl J Med. 2014; 370:1702–1711. [PubMed: 24678955]
27. O'Donoghue ML, Braunwald E, White HD, et al. Effect of darapladib on major coronary events after an acute coronary syndrome: the SOLID-TIMI 52 randomized clinical trial. JAMA. 2014; 312:1006–1015. [PubMed: 25173516]
28. Elkhawad M, Rudd JH, Sarov-Blat L, et al. Effects of p38 mitogen-activated protein kinase inhibition on vascular and systemic inflammation in patients with atherosclerosis. JACC Cardiovasc Imaging. 2012; 5:911–922. [PubMed: 22974804]
29. Emani H, Vucic E, Subramanian S, et al. The effect of BMS-582949, a p38 mitogen-activated protein kinase (p38 MAPK) inhibitor on arterial inflammation: a multicentre FDG-PET trial. Atherosclerosis. 2015; 240:490–496. [PubMed: 25913664]
30. O'Donoghue ML, Glaser R, Cavender MA, et al. Effect of losmapimod on cardiovascular outcomes in patients hospitalized with acute myocardial infarction: a randomized clinical trial. JAMA. 2016; 315:1591–1599. [PubMed: 27043082]
31. Sakalihasan N, Van Damme H, Gomez P, et al. Positron emission tomography (PET) evaluation of abdominal aortic aneurysm (AAA). Eur J Vasc Endovasc Surg. 2002; 23:431–436. [PubMed: 12027471]
32. Morel O, Mandry D, Micard E, Kauffmann C, Lamiral Z, Verger A, et al. Evidence of cyclic changes in the metabolism of abdominal aortic aneurysms during growth phases: a FDG-PET sequential observational study. J Nucl Med. 2015; 19:114.
33. Rudd JH, Coughlin PA, Groves A. Predicting aortic aneurysm expansion by PET. J Nucl Med. 2015; 23:115.
34. Stacy MR, Zhou W, Sinusas AJ. Radiotracer imaging of peripheral vascular disease. J Nucl Med. 2013; 54:2104–2110. [PubMed: 24101686]
35. Myers KS, Rudd JH, Haliman EP, et al. Correlation between arterial FDG uptake and biomarkers in peripheral artery disease. JACC Cardiovasc Imagining. 2012; 5:38–45.
36. Silvera SS, Aidi HE, Rudd JH, et al. Multimodality imaging of atherosclerotic plaque activity and composition using FDG-PET/CT and MRI in carotid and femoral plaques. Atherosclerosis. 2009; 207:139–143. [PubMed: 19467659]
37. Doherty TM, Asotra K, Fitzpatrick LA, et al. Calcification in atherosclerosis: bone biology and chronic inflammation at the arterial crossroads. Proc Natl Acad Sci USA. 2003; 100:11201–11206. [PubMed: 14500910]
38. Schenker MP, Dorbala S, Hong EC, et al. Interrelation of coronary calcification, myocardial ischemia, and outcomes in patients with intermediate likelihood of coronary artery disease: a combined positron emission tomography/computed tomography study. Circulation. 2008; 117:1693–1700. [PubMed: 18362235]
39. Bos D, Leening MJ, Kavousi M, et al. Comparison of atherosclerotic in major vessel beds on the risk of all-cause and cause-specific mortality: The Rotterdam Study. Circ Cardiovasc Imaging. 2015; 8:e003843. [PubMed: 26659376]
40. Hawkins RA, Choi Y, Huang SC, et al. Evaluation of the skeletal kinetics of fluorine-18-fluoride ion with PET. J Nucl Med. 1992; 33:633–642. [PubMed: 1569473]
41. Grant FD, Fahey FH, Packard AB, et al. Skeletal PET with 18 F-fluoride: applying new technology to an old tracer. J Nucl Med. 2008; 49:68–78. [PubMed: 18077529]
42. Aikawa E, Nahrendrof M, Figueiredo JL, et al. Osteogenesis associates with inflammation in early-stage atherosclerosis evaluated by molecular imaging in-vivo. Circulation. 2007; 116:2841–2850. [PubMed: 18040026]
43. Derlin T, Toth Z, Papp L, et al. Correlation of inflammation assessed by 18F-FDG PET, active mineral deposition assessed by 18F-fluoride PET, and vascular calcification in atherosclerotic plaque: a dual-tracer PET/CT study. J Nucl Med. 2011; 52:1020–1027. [PubMed: 21680686]
44. Abdelbaky A, Corsini E, Figueroa AL, et al. Focal arterial inflammation precedes subsequent calcification in the same location: a longitudinal FDG-PET/CT study. Circ Cardiovasc Imaging. 2013; 6:747–754. [PubMed: 23833282]

45. Derlin T, Richter U, Bannas P, et al. Feasibility of 18F-sodium fluoride PET/CT for imaging of atherosclerotic plaque. J Nucl Med. 2010; 51:862–865. [PubMed: 20484438]

46. Dweck MR, Chow MM, Joshi NV, et al. Coronary arterial 18F-sodium fluoride uptake: a novel marker of plaque biology. J Am Coll Cardiol. 2012; 59:1539–1548. [PubMed: 22516444]

**47. Joshi NV, Vesey AT, Williams MC, et al. 18F-fluoride positron emission tomography for identification of ruptured and high-risk coronary atherosclerotic plaques: a prospective clinical trial. Lancet. 2014; 383:705–713. 18F-NaF PET can noninvasively identify and localise ruptured and high-risk coronary plaque compared to non-culprit areas (TBR 1.66 vs. 1.24, $p < 0.001$, respectively). [PubMed: 24224999]

48. Fiz F, Morbelli S, Piccardo A, et al. 18F-NaF uptake by atherosclerotic plaque on PET/CT imaging: inverse correlation between calcification density and mineral metabolic activity. J Nucl Med. 2015; 56:1019–1023. [PubMed: 25952737]

*49. Irkle A, Vesey AT, Lewis DY, et al. Identifying active vascular microcalcification by (18)F-sodium fluoride positron emission tomography. Nat Commun. 2015; 6:7495. 18F-NaF adsorbs to calcific deposits within plaque and has a high affinity, being both selective and specific, and can distinguish between macro- and micro-calcification. [PubMed: 26151378]

50. Rominger A, Saam T, Vogl E, et al. In vivo imaging of macrophage activity in the coronary arteries using 68Ga-DOTATATE PET/CT: correlation with coronary calcium burden and risk factors. J Nucl Med. 2010; 51:193–197. [PubMed: 20080898]

51. Li X, Samnick S, Lapa C, et al. 68Ga-DOTATATE PET/CT for the detection of inflammation of large arteries: correlation with 18F-FDG, calcium burden and risk factors. EJNMMI Res. 2012; 2:52. [PubMed: 23016793]

52. Pederson SF, Sandholt BV, Keller SH, et al. 64Cu-DOTATATE PET/MRI for detection of activated macrophages in carotid atherosclerotic plaques: studies in patients undergoing endarterectomy. Arterioscler Thromb Vasc Biol. 2015; 35:1696–1703. [PubMed: 25977567]

53. Malmberg C, Ripa RS, Johnbeck CB, et al. 64Cu-DOTATATE for noninvasive assessment of atherosclerosis in large arteries and its correlation with risk factors: head-to-head comparison with 68Ga-DOTATOC in 60 patients. J Nucl Med. 2015; 56:1895–1900. [PubMed: 26429961]

54. Bird, Jl, Izquierdo-Garcia, D., Davies, JR., et al. Evaluation of translocator protein quantification as a tool for characterising macrophage burden in human carotid atherosclerosis. Atherosclerosis. 2010; 210:388–391. [PubMed: 20056222]

55. Gaemperli O, Shalhoub J, Owen DR, et al. Imaging intraplaque inflammation in carotid atherosclerosis with 11C-PK11195 positron emission tomography/computed tomography. Eur Heart J. 2010; 33:1902–1910.

56. Tahara N, Mukherjee J, de Haas HJ, et al. 2-deoxy-2-[18F]fluoro-D-mannose positron emission tomography imaging in atherosclerosis. Nat Med. 2014; 20:215–219. [PubMed: 24412923]

57. Kooi ME, Cappendijk VC, Cleutjens KB, et al. Accumulation of ultrasmall superparamagnetic particles of iron oxide in human atherosclerotic plaques can be detected by in vivo magnetic resonance imaging. Circulation. 2003; 107:2453–2458. [PubMed: 12719280]

58. Tang TY, Howart SP, Miller SR, et al. The ATHEROMA (Atorvastatin Therapy: Effects on reduction of Macrophage Activity) Study. Evaluation using ultrasmall superparamagnetic iron oxide enhanced magnetic resonance imaging in carotid disease. J Am Coll Cardiol. 2009; 53:2039–2050. [PubMed: 19477353]

59. Alam SR, Shah AS, Ricahrds J, et al. Ultrasmall superparamagnetic particles of iron oxide in patients with acute myocardial infarction: early clinical experience. Circ Cardiovasc Imaging. 2012; 5:559–565. [PubMed: 22875883]

60. McBride OM, Joshi NV, Robson JM, et al. Positron emission tomography and magnetic resonance imaging of cellular inflammation in patients with abdominal aortic aneurysms. Eur J Vasc Endovasc Surg. 2016; 51:518–526. [PubMed: 26919936]

61. Mulder WJ, Jaffer FA, Fayad ZA, et al. Imaging and nanomedicine in inflammatory atherosclerosis. Sci Transl Med. 2014; 6:239sr1. [PubMed: 24898749]

62. Jaffer FA, Verjans JW. Molecular imaging of atherosclerosis: clinical state-of-the-art. Heart. 2014; 100:1469–1477. [PubMed: 24365664]

63. Bourantas CV, Jaffer FA, Gijsen FJ, et al. Hybrid intravascular imaging: recent advances, technical considerations, and current applications in the study of plaque pathophysiology. Eur Heart J. 2016 [Epub ahead of print].

*64. Ughi GJ, Wang H, Gerbaud E, et al. Clinical characterisation of coronary atherosclerosis with dual-modality OCT and near infrared autofluorescence imaging. JACC cardiovasc Imaging. 2016 [Epub ahead of print]. First-in-human study of intravascular OCT and near-infrared fluorescence imaging of coronary atherosclerosis.

65. Jaffer FA, Vinegoni C, John MC, et al. Real-time catheter molecular sensing of inflammation in proteolytically active atherosclerosis. Circulation. 2008; 118:1802–1809. [PubMed: 18852366]

66. Jaffer FA, Calfon MA, Rosenthal A, et al. Two-dimensional intravascular near-infrared fluorescence molecular imaging of inflammation in atherosclerosis and stent-induced vascular injury. J Am Coll Cardiol. 2011; 57:2516–2526. [PubMed: 21679853]

67. Khamis RY, Wollard KJ, Hyde GD, et al. Near infrared fluorescence (NIRF) molecular imaging of oxidized LDL with an autoantibody in experimental atherosclerosis. Sci Rep. 2016; 26:21785.

68. Vinegoni C, Botnaru I, Aikawa E, et al. Indocyanine green enables near-infrared fluorescence imaging of lipid-rich, inflamed atherosclerotic plaques. Sci Transl Med 2011. 2011; 3:84ra45.

*69. Verjans JW, Osborn EA, Ughi GJ, et al. Targeted near-infrared fluorescence imaging of atherosclerosis: clinical and intracoronary evaluation of indocyanine green. JACC Cardiovasc Imaging. 2016 [Epub ahead of print]. Subsequent clinical study of indocyanine green NIRF imaging demonstrated that ICG targets human plaques in areas of impaired endothelial barrier function. ICG may accelerate first-in-human intravascular NIRF molecular imaging studies.

*70. Yoo H, Kim JW, Shishkov M, et al. Intra-arterial catheter for simultaneous microstructural and molecular imaging in vivo. Nat Med. 2011; 17:1680–1684. First combined intravascular molecular-structural imaging system, using NIRF-OCT. [PubMed: 22057345]

71. Hara T, Ughi GJ, McCarthy JR, et al. Intravascular fibrin molecular imaging improves the detection of unhealed stents assessed by optical coherence tomography in vivo. Eur Heart J. 2015 [Epub ahead of print].

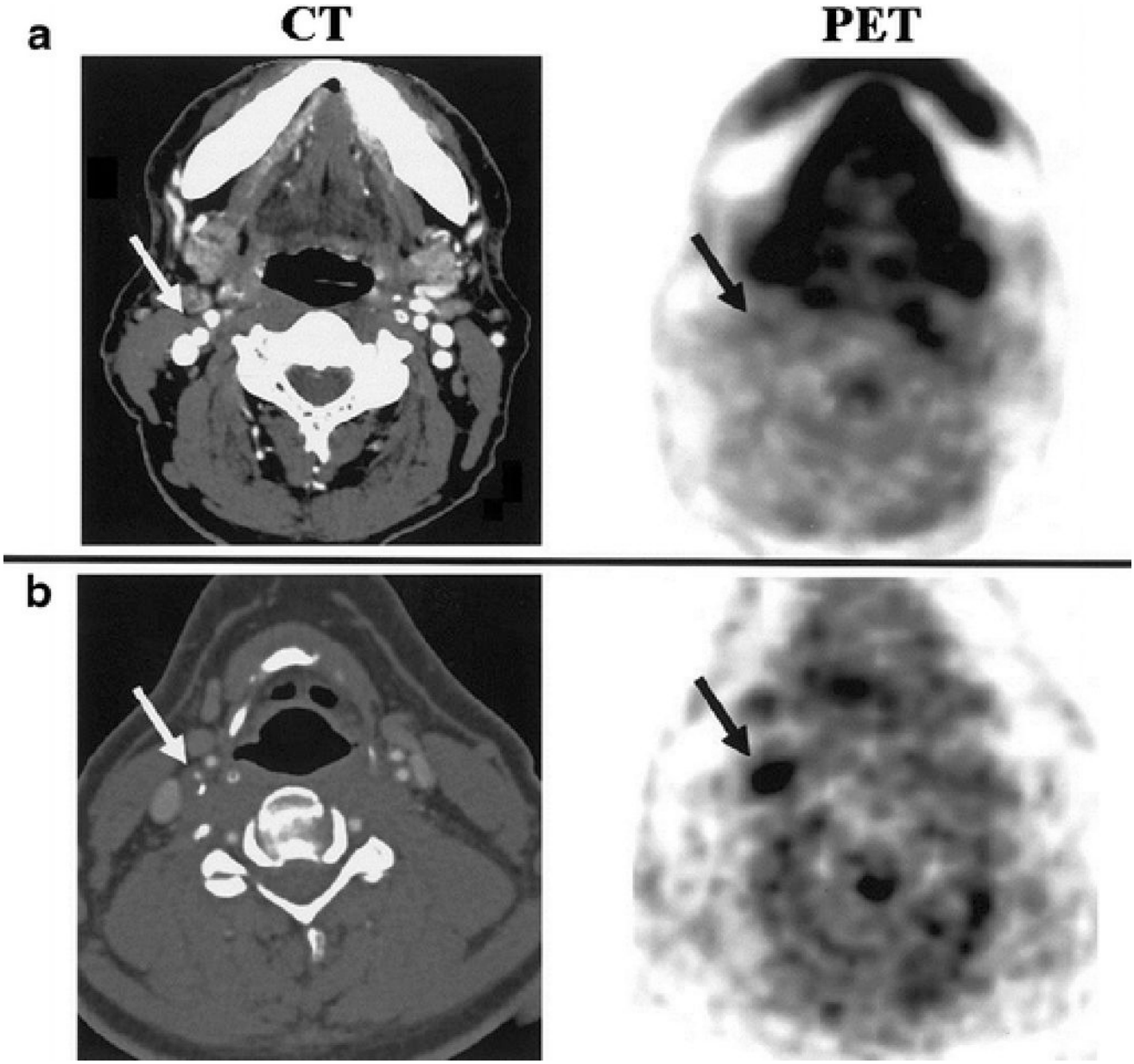

Figure 1.

FDG uptake in carotid plaques of patients. Axial images of both CT and PET data from a patient with low (PET A) and high (PET B) FDG uptake in the region of the internal carotid artery (arrows). FDG was associated with histological plaque macrophages, a key inflammatory cell driver of plaque complications. Reproduced by permission from reference (6).

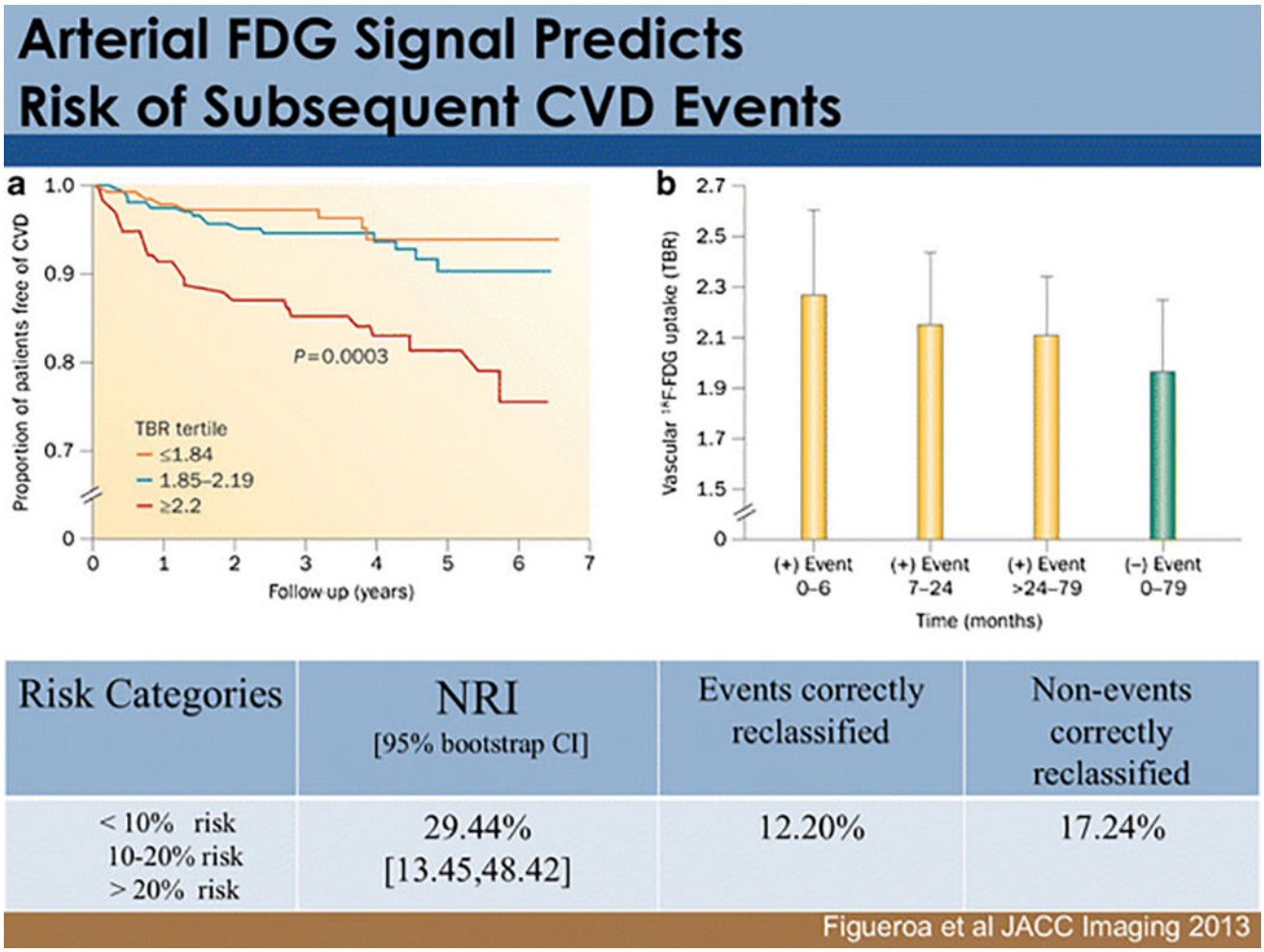

Figure 2.

Arterial FDG uptake associates with the risk of subsequent CVD events. **A)** A study of 519 individuals without active cancer or pre-existing cardiovascular disease found that those with high aortic FDG uptake (the highest tertile of activity) were subsequently found to have a substantially increased risk of CVD, which remained independently predictive after adjusting for Framingham Risk Score or Coronary Calcium Score. **B**) The baseline arterial FDG signal also related to the timing of the subsequent event, whereby those with highest signals had events that occurred earlier than those with intermediate arterial FDG signals. Reproduced by permission from reference (15).

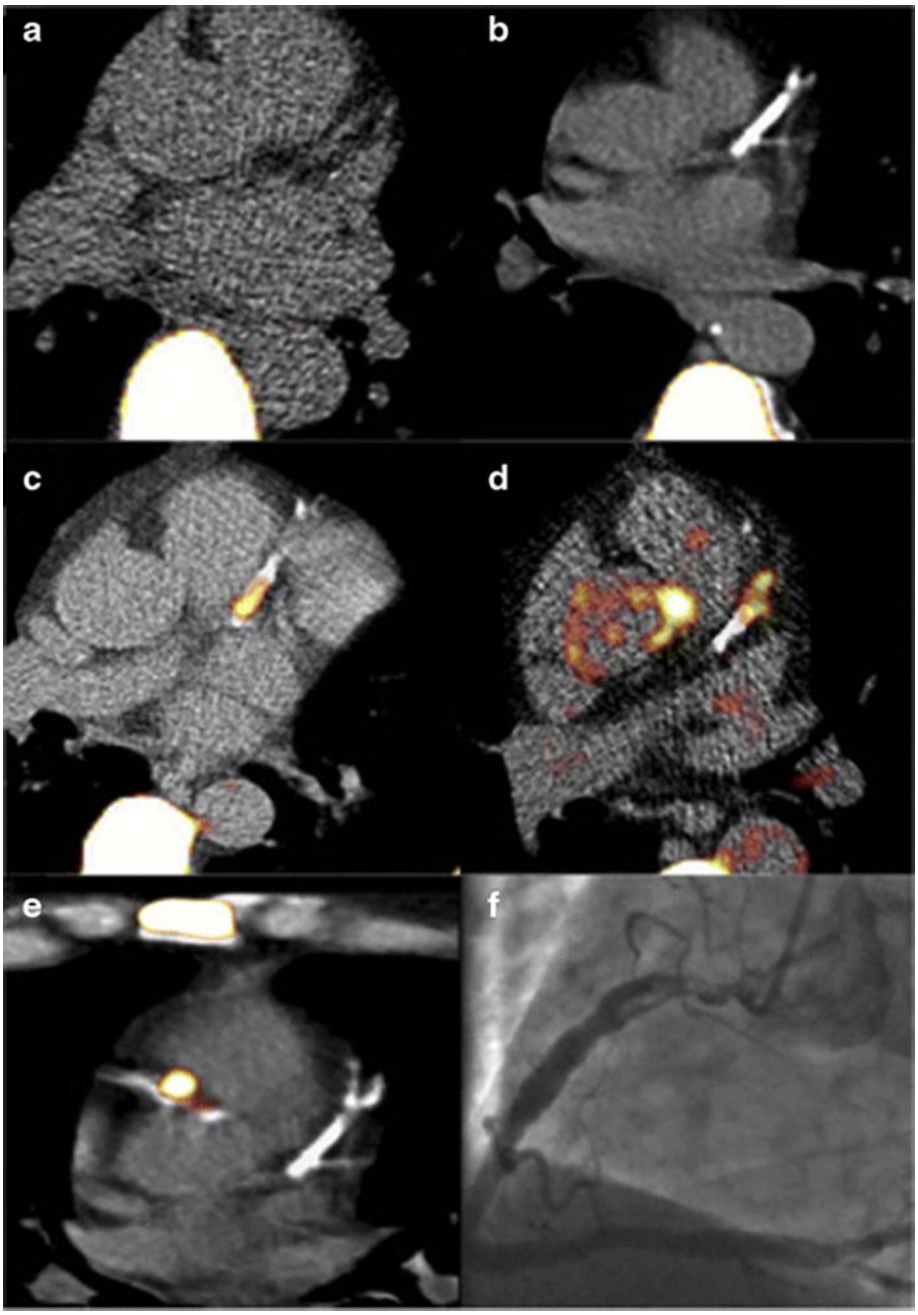

Figure 3.

Molecular imaging of coronary plaque osteogenesis via 18F-NaF PET imaging fused with coronary CT images. (A) Control patient with little coronary calcification or 18F-NaF uptake. (B) The panel demonstrates extensive coronary calcification without significant 18F-NaF uptake. (C and D) Focal NaF uptake in the LAD with flanking coronary arterial calcification. (E) Patient with a NSTEMI showing focal 18F-NaF tracer uptake in culprit lesion with (F) associated in-situ thrombus in the proximal right coronary artery. Reproduced by permission from reference (45).

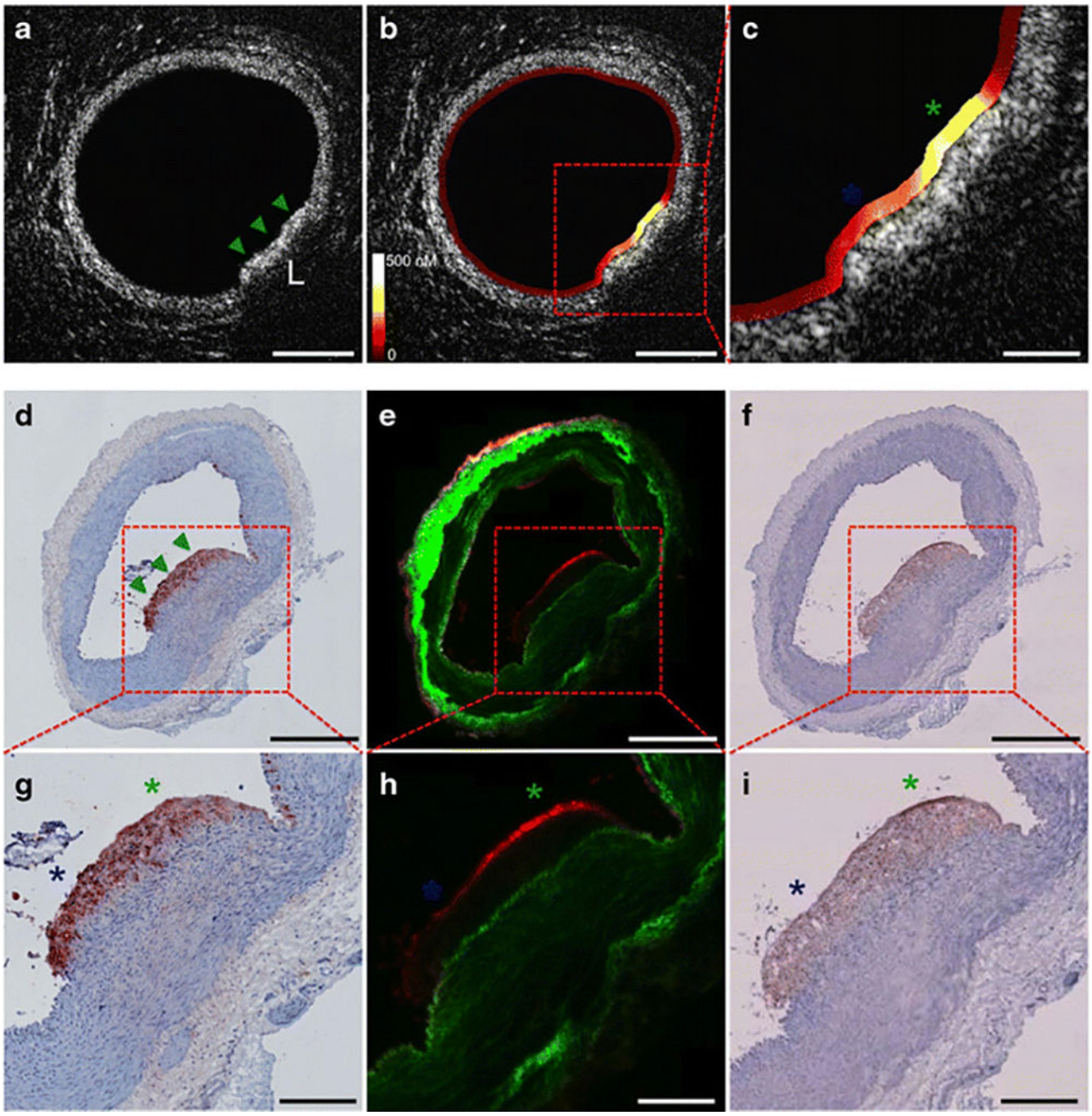

Figure 4.

High-resolution intravascular NIRF-OCT molecular-structural imaging of inflammatory protease activity in rabbit atherosclerosis. (a–c) Cross-sectional NIRF-OCT imaging of normal artery wall (a) and an atherosclerotic lesion (b,c), lipid-rich demonstrated by green and blue asterisks. (d–f) RAM-11 macrophage staining of plaque sections demonstrating high macrophage density, fluorescence microscopy with elevated plaque protease activity and positive cathepsin immunostain signal. (g–i) higher magnification of images d–f. Reproduced by permission from reference (70).